

Back-in-Time Diffusion: Unsupervised Detection of Medical Deepfakes

FRED M. GRABOVSKI, Ben-Gurion University, BGU

LIOR YASUR, Ben-Gurion University, BGU

GUY AMIT, Ben-Gurion University, BGU

YISROEL MIRSKY*, Ben-Gurion University, BGU

Recent progress in generative models has made it easier for a wide audience to edit and create image content, raising concerns about the proliferation of deepfakes, especially in healthcare. Despite the availability of numerous techniques for detecting manipulated images captured by conventional cameras, their applicability to medical images is limited. This limitation stems from the distinctive forensic characteristics of medical images, a result of their imaging process.

In this work we propose a novel anomaly detector for medical imagery based on diffusion models. Normally, diffusion models are used to generate images. However, we show how a similar process can be used to detect synthetic content by making a model reverse the diffusion on a suspected image. We evaluate our method on the task of detecting fake tumors injected and removed from CT and MRI scans. Our method significantly outperforms other state of the art unsupervised detectors with an increased AUC of 0.9 from 0.79 for injection and of 0.96 from 0.91 for removal on average. We also explore our hypothesis using AI explainability tools and publish our code and new medical deepfake datasets to encourage further research into this domain.

CCS Concepts: • **Computing methodologies** → **Anomaly detection**; *Machine learning approaches*; • **Applied computing** → **Health informatics**; • **General and reference** → Validation.

Additional Key Words and Phrases: medical deepfakes, diffusion models, anomaly detection, unsupervised learning, MRI, CT scans

ACM Reference Format:

Fred M. Grabovski, Lior Yasur, Guy Amit, and Yisroel Mirsky. 2024. Back-in-Time Diffusion: Unsupervised Detection of Medical Deepfakes. 1, 1 (October 2024), 18 pages. <https://doi.org/10.1145/nnnnnnn.nnnnnnn>

1 Introduction

In recent years, the field of generative AI has gained increasing popularity with the introduction of Generative Adversarial Networks (GANs) and diffusion models which are capable of generating and editing images with impressive quality. However, these models can be used maliciously to create ‘deepfakes’; believable media created by deep neural network [30]. Deepfakes can be used to spread misinformation [2, 21], manipulate forensic evidence [24], perform blackmail [22] and even perform scams [13].

*Corresponding Author

Authors’ Contact Information: Fred M. Grabovski, freddie@post.bgu.ac.il, Ben-Gurion University, BGU; Lior Yasur, Ben-Gurion University, BGU, lartst@affiliation.org; Guy Amit, Ben-Gurion University, BGU; Yisroel Mirsky, Ben-Gurion University, BGU.

Permission to make digital or hard copies of all or part of this work for personal or classroom use is granted without fee provided that copies are not made or distributed for profit or commercial advantage and that copies bear this notice and the full citation on the first page. Copyrights for components of this work owned by others than the author(s) must be honored. Abstracting with credit is permitted. To copy otherwise, or republish, to post on servers or to redistribute to lists, requires prior specific permission and/or a fee. Request permissions from permissions@acm.org.

© 2024 Copyright held by the owner/author(s). Publication rights licensed to ACM.

ACM XXXX-XXXX/2024/10-ART

<https://doi.org/10.1145/nnnnnnn.nnnnnnn>

The proliferation of deepfakes can be attributed in-part to the growing accessibility of these technologies. Given the tools and online resources today, very little technical expertise is required to create a convincing deepfake. For example, with publicly available text-to-image models [10, 34], such as Stable Diffusion [35], anyone can easily create and edit image content using only textual instructions.

Deepfakes can also be applied to the healthcare sector. In a paper called CT-GAN [31] the authors demonstrated that malicious actors can gain access to records at a hospital and manipulate CT scans of patients with deepfake content. There are several reasons an adversary would want to perform a deepfake attack on medical imagery. For example, an attacker can add a small brain aneurysm to his/her own MRI scan as irrefutable evidence for losing the ability to taste, enabling the attacker to collect money from a quality of life insurance policy. Moreover, an attacker can alter political a candidate's medical records to affect elections or to harm individuals as a form of murder or assassination.

The threat of medical deepfakes is a notable concern because cyber adversaries can access private medical imagery. Numerous research papers and security reports have demonstrated that attackers can access and modify medical scans through cyberattacks and physical intrusions [1, 4, 12, 43]. Moreover, advances in generative AI enables adversaries to alter medical evidence in a medical scan with little effort or medical knowledge. For example, it can be used to hide the presence of a cancerous tumor to the degree of realism where both experienced radiologist and AI-tools can be deceived [31]. Moreover, in this paper we show how text-to-image models such as [35, 37], can be used to tamper medical imagery by tuning it with just a few images.

A challenge with using existing tamper detection models is that they are designed with the assumption that the images were captured using a conventional camera. Conventional cameras use CMOS (Complementary Metal-Oxide Semiconductor) or CCD (Charge-Coupled Device) imaging sensors which *linearly* maps received light to pixels in an image. This results in uniform noise patterns in the image which can be utilized to detect image tampering [25]. However, medical imaging devices capture images in a very different manner resulting in non-uniform forensic patterns. For example, CT scanner uses X-rays to capture multiple cross-sectional views of an object from different angles. These views are then processed using a radon transform to reconstruct the internal image (slice). As a result, many existing detection methods, such as [6–8, 14], cannot detect medical deepfakes very well (demonstrated in section 5).

Deep learning based anomaly detection is ideal for this setting because unsupervised techniques do not require labeled examples of tampered images; rather examples of benign images which are often plenty. Recent advances in generative AI has led to breakthroughs in this domain. Notably, it has been recently shown that Denoising Diffusion Probabilistic Models (DDPMs), which are normally used to generate images, can be used to detect anomalous images as well [11]. The general approach is to (1) train the DDPM on normal data, (2) noise the target image, (3) use the DDPM to denoise it and then (3) compare the denoised image to the original; if the size of their residual (i.e., their ℓ_2 distance) is high, then the target image is considered anomalous.

While the use of DDPMs can help overcome the issue of modeling medical forensics, there are two issues with existing techniques:

Content Divergence. In order to create a residual, existing methods add noise to the image before performing reconstruction. However, as we show in this paper, doing so causes two problems: (1) the DDPM produces novel and irrelevant semantic features which leads to false positives and (2) the magnitude of the added content overpowers subtle forensic patterns discovered in the residual. For example, any latent noise patterns from the imaging device and blending artifacts. While this approach works well when searching for anomalous

out of distribution content (e.g., an object that was not in the training dataset [17]) it harms the capability detecting subtle forensic evidence. Therefore, existing methods are not suitable for deepfake detection and possibly tamper detection in general.

Long Runtime. When using these techniques, the noised version of the image must be passed through the model multiple times until the noise has been removed. These models are often large and therefore the denoising process of a single image can take tens of seconds and even minutes. While this is not an issue when testing a single image, it is a critical one when applying this technique at scale (e.g., when scanning a clinic’s entire medical database for tampering).

To address this gap, we introduce a novel DDPM-based anomaly detection method called Back-in-Time Diffusion (BTD). Unlike past works, BTD directly denoises the target image without adding any noise. As a result, the BTD’s residual only contains anomalous forensic content. Furthermore, BTD only requires only a single step of diffusion, making it much faster than traditional DDPM processes.

To use BTD, the DDPM model is trained in an unsupervised manner on the target domain, such as random CT scans without tampered content, which eliminates the need for data labeling. This unsupervised approach makes the model practical and cost-effective to train, while also enabling it to generalize well to unseen deepfake technologies, making it robust against a wide variety of manipulation methods.

To thoroughly evaluate our method, we conducted extensive testing across numerous scenarios. We included both MRI and CT medical scans obtained from a diverse range of scanners, ensuring that our model can handle data variability inherent in different imaging devices. We specifically focused on detecting cancer injection and removal manipulations in breast and lung images, as the diagnosis of these conditions are critical. To simulate these deepfakes, we utilized two distinct medical deepfake technologies: CT-GAN and the a generative model based on Stable Diffusion. Finally, for detection we evaluated both conventional image forensic techniques, modern deep learning methods, and DDPM anomaly detectors.

Our results demonstrate that BTD significantly outperforms all other state-of-the-art detectors across every scenario. For detecting injection deepfakes, BTD achieved an AUC of 0.9, notably higher than the next best method, which only reached 0.79. Similarly, for detecting removal deepfakes, BTD achieved an AUC of 0.96, outperforming the next best method, which scored 0.91. Unlike competing approaches, which show inconsistent performance across different tasks, BTD consistently excels, making it the most robust and reliable detector in all tested cases.

To enable reproducibility of our work and encourage further research, we published our six novel deepfake datasets and source code online.¹

In summary our contributions are:

- A novel technique for detecting forensic anomalies in images, evaluated on various medical imaging modalities. The method outperforms other state-of-the-art techniques at detecting medical deepfakes.
- We have created and published six new medical deepfake evaluation datasets using state of the art techniques which the community can use as benchmarks.

2 Related Work

The exploration of tamper detection in images has evolved significantly, initially centering on conventional manipulation techniques like splicing and copy-move [7, 28, 41]. However, the advent

¹Code: <https://github.com/FreddieMG/BTD--Unsupervised-Detection-of-Medical-Deepfakes>
Datasets: <https://www.kaggle.com/datasets/freddiegraboski/btd-mri-and-ct-deepfake-test-sets/>

of advanced generative models such as GANs and diffusion models has shifted focus towards detecting images synthesized through deep learning [9, 15, 19].

Supervised approaches to deepfake detection necessitate extensive training datasets that cover all types of deepfakes [42, 45]. This is particularly challenging due to the rapid evolution of deepfake technology and the scarcity of comprehensive datasets, especially in the medical domain.

To counter this challenge, unsupervised learning techniques can be used. Two prevalent methods for detecting image anomalies in an unsupervised setting are: reconstruction-based approaches and fingerprint-based approaches.

Reconstruction-based approaches rely on modeling genuine image distributions and then identifying samples that deviate from them. For example an autoencoder (AE) or Vision Transformer (ViT) can be used to detect manipulated images by identifying cases where the model fails to reconstruct the same image (indicating an outlier) [11, 36, 47]. Such methods compress and reconstruct the entire image, potentially smoothing over subtle distortions, unlike BTM which effectively captures these distortions by strategically applying only a small number of backward steps in the diffusion process. This approach meticulously peels back the layers of noise added during image manipulation, revealing underlying discrepancies. Using this method, BTM exposes potential tampering, making it adept at identifying manipulations that other methods might miss due to their broader reconstruction approach.

Other methods using diffusion models have also been adapted to the task of anomaly detection. For example, the authors of [16, 17, 26] utilize these models by performing forward diffusion and backward diffusion, and then by comparing the source image to the reconstructed image. In contrast, BTM only utilizes the backward diffusion for a single step, resulting in faster inference. Furthermore, while these methods perform well at detecting anomalous samples (e.g., novel objects), they perform poorly in the task of detecting image tampering. This is because their backward diffusion process starts from a noisy sample which causes the DDPM to add novel and irrelevant patterns and content to the image. In contrast, BTM extracts the subtle forensic patterns by immediately performing backwards diffusion on the sample, enabling it to detect tampering attacks much better.

Finally, some works suggest using conditional diffusion models for specific anomaly detection tasks [32, 44]. However, compared to BTM, these approaches are supervised, making them impractical for detecting medical deepfakes. This is because it would require curating and maintaining an up to date large scale medical deepfake dataset.

Classic forensic methods are a common choice for image tamper detection. The popular approach is to search the media for the latent noise pattern left by the imaging device. Tampering is detected if the latent noise pattern has been disturbed due to blending (splicing) or removed due to synthesized content [5, 6, 29]. These approaches assume that images contain uniform noise patterns left by the imaging sensor [5, 8, 14]. However, the imaging processes of medical devices (such as MRI and CT) is different than in standard cameras for which these algorithms were designed. For example, CT and MRI scanners have an imaging head that spins around the object while performing radial integrals to visualize the object volume; a process which results in *non-uniform* latent noise patterns.

Other works offer methods for detecting tampering by comparing an image to its metadata such as exposure and ISO settings [21]. Unfortunately, these approaches cannot be directly applied to medical imagery. In contrast, our Back-in-Time Diffusion (BTM) technique leverages the unsupervised potential of Denoising Diffusion Probabilistic Models (DDPMs) to offer a versatile solution for detecting manipulated images, bypassing the limitations of existing methods in the medical domain and in additional scenarios in which the imaging process is different or the availability of image meta data is limited.

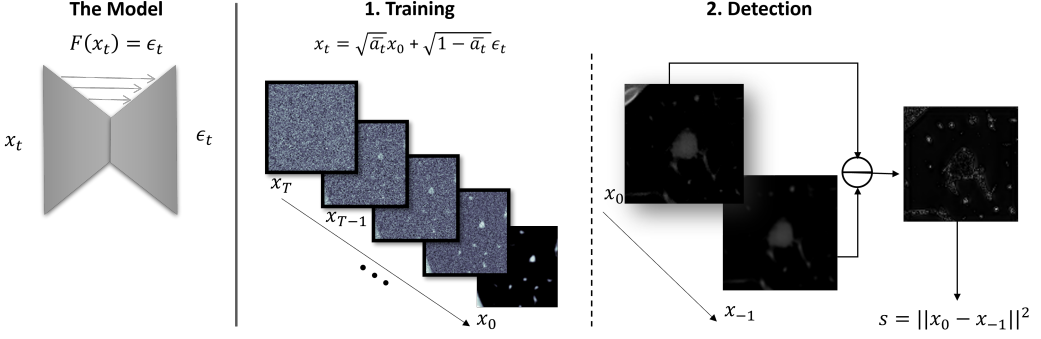


Fig. 1. Overview of the Back-in-Time Diffusion framework. The model is a U-net that predicts the noise added in the last step ($F(x_t) \Rightarrow \epsilon_t$). The model is trained by progressively adding noise to the images (x_0) to generate noisy versions (x_t) and then learning to predict the noise added at each step. Detection is performed on image x_0 by measuring the error after d steps.

3 Back-In-Time Diffusion

3.1 Diffusion Models

Denoising diffusion probabilistic models (DDPM) [19] are a class of generative models which are inspired by concepts from nonequilibrium thermodynamics.

DDPMs utilize two processes (1) forward diffusion, which is the process of noising an input sample $x_0 \sim q(x_0)$ into a noise $x_T \sim \mathcal{N}(0, I)$, and (2) the backward diffusion process, that reverses the forward diffusion process, from x_T to x_0 using T time steps.

The training of DDPMs is an iterative process, where in each iteration, a random number of steps t is selected, and the forward diffusion process is used to noise an input sample x_0 into x_t over t steps using a closed mathematical formula

$$x_t = \sqrt{\bar{\alpha}_t} \cdot x_0 + \sqrt{1 - \bar{\alpha}_t} \cdot \epsilon_t \quad (1)$$

where $\epsilon_t \sim \mathcal{N}(0, I)$ and $\bar{\alpha}_t = \prod_{i=1}^t \alpha_i$ is a term responsible for controlling the image content loss in each time step of the forward process. After the noised sample x_t is calculated, the backward diffusion process uses a U-Net-like [39] neural network $F(x_t)$ to estimate the noise ϵ between x_t and x_{t-1} . The neural network is then updated according to a gradient step minimizing the squared difference between the noise ϵ_t and the neural network output $F(x_t)$:

$$loss = ||\epsilon_t - F(x_t)||^2 \quad (2)$$

Finally, after the neural network's training has converged, the backward diffusion process can be used to generate new images. The process starts from noise $\epsilon \sim \mathcal{N}(0, I)$ and then repeatedly estimates x_{t-1} from x_t , until $t = 0$, resulting in a sample x_0 similar to samples in the training set. More details about diffusion models can be found at [10, 19].

3.2 The Problem with Existing DDPM Anomaly Detection

Let x_0 be a target image which we want to examine for anomalies. Existing DDPM anomaly detectors work by using the DDPM process to remove anomalous features and then by comparing the result. The process is to first train a DDPM *on authentic images only*. Then the DDPM is used to determine if x_0 is anonymous by following three steps:

- (1) *Forwards diffusion*. x_0 is noised k steps to remove the anomalous content.

- (2) *Backwards diffusion.* x_k is denoised k steps to produce x'_0 ; the reconstruction of x_0 without anomalous content.
- (3) *Residual.* The magnitude of the residual $\|x_0 - x'_0\|^2$ is computed to quantify the anomalous content in x_0 .

The intuition is that since the backwards diffusion model was only trained on benign content, it will only be able to repair x_k with normal features. As a result, the residual will capture what is anomalous w.r.t. the training distribution.

The problem with this process is that the forwards diffusion steps add add to the image. This encourages the backward diffusion process to create novel and irrelevant content to the image. This leads to increased false positives and the inability to measure the presence of subtle forensics because the magnitude of these novel features.

3.3 The Proposed Approach (BTD)

In order to avoid the issue of generating irrelevant content, we instead opt for utilizing DDPMs to identify subtle forensics left in the image from the tampering process. Examples of these forensics include, blending boundaries and inconsistent latent noise patterns [33, 40, 41].

To accomplish this, we do not add any noise to x_0 but rather perform a single denoising step directly to it. By doing so, the model attempts to correct the latent noise patterns to make them appear more similar to samples from the training set. As a result, the residual captures *anomalous* noise patterns apparent in the image. Therefore, the BTD process has two steps in total (illustrated in Figure 1):

- (1) *Backwards diffusion.* Target image x_0 is denoised for one step obtaining x_{-1} .
- (2) *Residual.* The magnitude of the residual $\|x_0 - x_{-1}\|^2$ is computed to quantify the anomalous content in x_0 . A larger residual indicates a higher likelihood that the image contains anomalous noise patterns.

While it is possible to continue the backward diffusion process further than one step, we found that doing so harms performance. This is because doing so harms both the benign subtle features and eventually benign foreground features; leading to false positives.

Since by definition $F(x_0) \approx x_{-1} - x_0$, the entire process can be summarized as

$$s = \|F(x_0)\|^2 \quad (3)$$

where $s \in [0, \infty)$ is the anomaly score.

For medical deepfakes, we found that when content (i.e., tumors) are injected into a scan, it is beneficial to focus on the residual around the tampered area itself. Therefore, when looking for injected content, we take the average around the area of interest. Specifically, we take the average of the residual 32x32 patch around the center of the tumor.

3.4 Calibrating BTD

The identification of fake samples is performed by flagging samples that obtain an anomaly score greater than some predetermined threshold τ :

$$p(\text{score}) = \begin{cases} \text{Real} & \text{if } \tau \leq s \\ \text{Fake} & \text{if } \tau > s \end{cases} \quad (4)$$

The threshold τ can be determined statistically in an unsupervised manner: first we compute the anomaly scores of benign images that were not used to train F . Then fit the distribution to a CDF and set the τ such that the probability of a false positive is sufficiently low.

3.5 Detection Stability

DDPMs are known for their stochastic nature, attributed to the random noise sampled during the backward diffusion process. Deploying a DDPM based detection tool may raise some understandable concerns regarding the stability and reproducibility of detection performance. However, in our experiments we have found that since we only take one backwards step, there is a negligible variance in reconstruction results. Therefore, BTM can offer reliable results.

4 Experiment Setup

In this section, we describe how we evaluated BTM's ability to detect deepfakes. For reproducibility, we have made the the source code of BTM and the datasets used in this paper available online.² Attack Scenarios. We considered different medical modalities, attacks scenarios and medical deepfake technologies:

For the modalities, we examined cancerous tumors in CT lung and MRI breast scans. For the attack scenarios, we analyzed the injection and removal of tumors. In the case of injection, samples representing authentic images with malignant tumors are called True-Malign (TM) samples, and those with artificially inserted malignant tumors are called Fake-Malign (FM) samples. Similarly, for removal, True-Benign (TB) samples are genuine benign images and Fake-Benign (FB) samples are images with artificially removed tumors. For the medical deepfake technologies, we used CT-GAN from [31] which performs volumetric in-painting and Stable Diffusion (SD) from [35, 37] to tamper the images. We implemented the SD injection attack by fine-tuning a Stable Diffusion model specifically on malignant slices (one for each modality). For the removal of tumors using Stable Diffusion, we utilized an "off-the-shelf" model without the need for additional fine-tuning. To the best of our knowledge, this is the first work that demonstrates the use of SD for creating medical deepfakes.

4.1 Datasets

To create our datasets we first collected authentic TM and TB images from the Duke Breast Cancer MRI dataset [38] and the LIDC [3] datasets. MRI images were standardized on a per-patient basis and CT images were clipped between -700 (Air) and 2000 (Bone). Both image modalities were then scaled to a [0, 1] range. Next, we preprocessed the datasets by cropping the imagery around regions of interest. For the TM dataset, this involved focusing on annotated tumor areas, while for the TB dataset, healthy tissue regions were randomly selected from the list of tumor locations to reflect the potential for containing a tumor. We then split these datasets into two portions: one for training BTM and a hold-out set both used for validating BTM and tuning the medical deepfake models (Stable Diffusion).

Utilizing the images in the hold-out set, we compiled six datasets for the evaluation: CTGAN-CT-Inject, CTGAN-CT-Remove, SD-CT-Inject, SD-CT-Remove, SD-MRI-Inject, and SD-MRI-Remove. These datasets consist of images from five different CT scanners and four MRI scanners. Sample images from our datasets are provided in Figure 3 where we show the before and after of applying the attacks. In Figure 2 we provide distribution of these data sets.

In total, we use 77K CT slices and 47K MRI slices for training, and for validation, we use 17K CT slices and 14K MRI slices. To avoid bias, the split was done according to patient. The train and validation sets only contained true samples (TB, TM) while the test sets contained a mix (TB, TM, FM and FB). The detectors were then trained using the train and validation sets and then evaluated on the respective test sets.

²<https://github.com/FreddieMG/BTD--Unsupervised-Detection-of-Medical-Deepfakes>
<https://www.kaggle.com/datasets/freddiegraboski/btd-mri-and-ct-deepfake-test-sets>

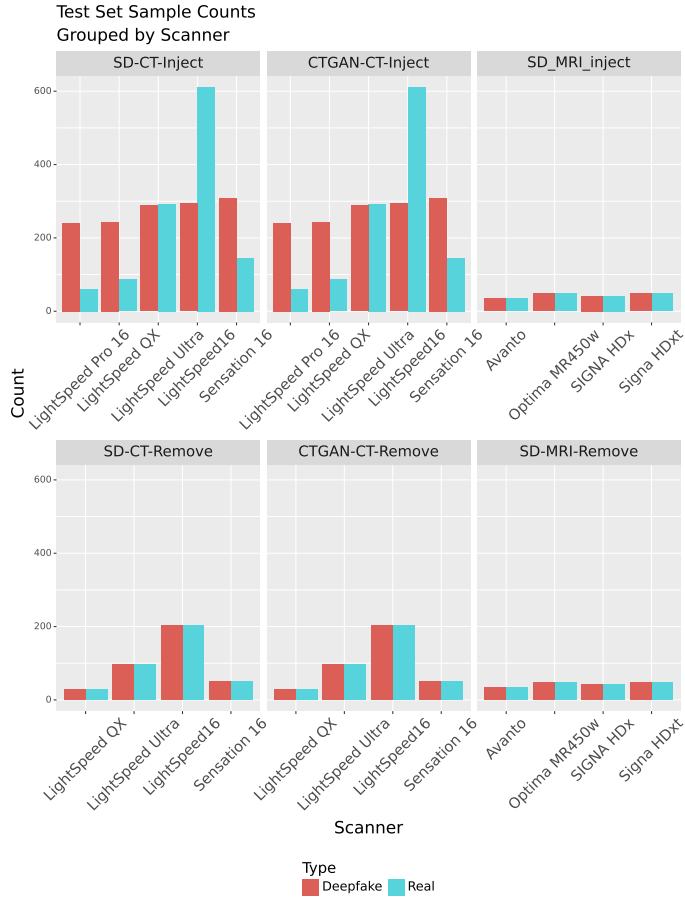


Fig. 2. The number of samples from each imaging device, per dataset.

4.2 BTD Configuration

Our framework revolves around a UNET-based Diffusion model, for which we used the default hyper-parameters,³ with the exception of the model's dimensions and batch size, which we changed to 32 `init_features` and 64 respectively. To apply BTB, we first extract a patch around the area of interest and then pass it through our model. We set the patch sizes to 96x96 and 128x128 for CT and MRI respectively to encapsulate potential tumors with sufficient context.

4.3 Baselines

Not all detection methods are applicable to our setup. To ensure a fair comparison, we only used methods that (1) train their model in an unsupervised manner, and (2) do not require additional metadata that is typically unavailable in medical imaging datasets. We compare BDT to the following methods:

Autoencoder Variants. AEs are frequently used for image anomaly detection tasks [46]. In general, when using AEs for image anomaly detection tasks, the original image is compared to

³<https://github.com/lucidrains/denoising-diffusion-pytorch>

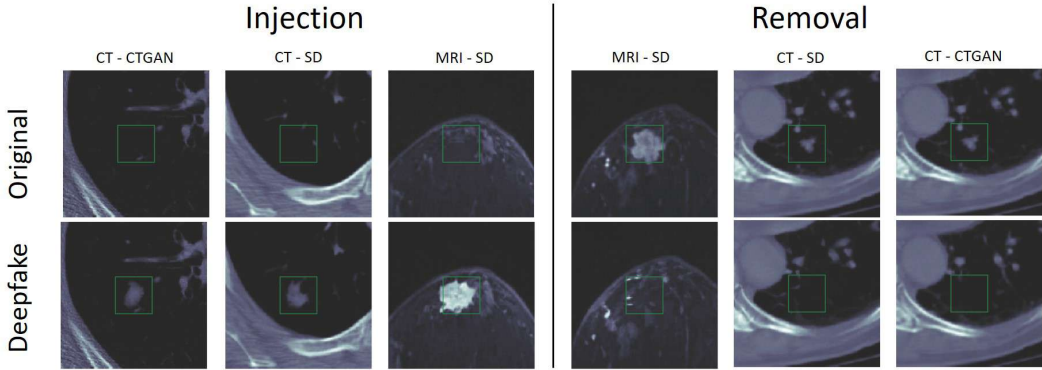


Fig. 3. Examples of manipulated images from our detection datasets. Top: original images. Bottom: images after being edited by generative models

its reconstructed version resulting in a map which localizes anomalous regions. We adopted four variants of AEs in our evaluation:

- AE [47] - A standard convolutional AE with 4 encoder and 4 decoder layers.
- U-net [36] - An AE based on the U-net architecture, with 16 *init_features*.
- In-paint AE [18] - An in-painting AE for anomaly detection. During inference, the center part of the image is masked and the AE attempts to complete it.
- OC-VAE [23] - A Variational AE architecture that was originally proposed for detecting fake face images.

Splice Buster. [7] A common baseline in the field of image forensics. This technique segments images into smaller sections and isolates the inherent noise present in each segment during the imaging procedure. These segments are subsequently grouped based on their distinctive noise patterns using a Gaussian Mixture Model, leading to two categories: benign and fake. The assigned probabilities for each segment are then employed to construct a heat map that indicates the likelihood of each pixel within the image being counterfeit.

Splice Radar. [14]: An advanced method in image forensics, utilizing a deep neural network (DNN). The approach involves training the DNN to grasp image characteristics, specifically the image fingerprint. This is accomplished by instructing the DNN to differentiate between the source imaging devices of the training images. Notably, the initial layer of the DNN is restricted to capturing solely high-frequency attributes from the image input. After training the DNN, it extracts representations for individual image segments. These representations are then inputted into a Gaussian Mixture Model, which clusters the segments into groups similar to SpliceBuster's technique.

Satellite ViT. [11, 20]: Designed to detect image manipulations using Vision Transformers (ViT) [11]. The fundamental concept driving this approach is rooted in the distinction of derivative patterns between benign and fake images. To this end, the method employs a ViT which is used as an AE. For every given input image, a comparison is performed between its derivative and the ViT's output corresponding derivative, facilitating the generation of a heat map that indicates the specific areas containing fake content within the image. We calculate thresholds from the validation sets of CT and MRI to keep only the more 'active' sections of the heat map and sum to calculate an anomaly score

OOD DDPM. [17]: An Out-of-distribution (OOD) detection method based on DDPMs. It detects anomalies by (1) reconstructing the target image from varying noise levels and then (2) by measuring the residuals of the reconstructions. Higher errors suggest the input differs from the training data, indicating an anomaly. In contrast to BTM, this detector must add noise to the images to perform the detection process.

All the methods in the evaluation were applied to our data datasets. We have used the author's code wherever possible, and in cases where the code was not available, we managed to get in touch with the authors in order to reproduce their work correctly.

Two models were trained for each method, one for CT and one for MRI. Each model was trained using benign and malignant image slices without tampered content.

4.4 Metrics

Performance was measured using area under the curve (AUC) and equal error rate (EER). For AUC, a larger value is better where 1.0 and 0.5 indicate perfect classification and random guessing respectively. For EER, a lower value indicates better performance. Our evaluation metrics are calculated using bootstrap sampling with 100 iterations, where in each iteration the number of samples per class were balanced across the scanners in the dataset. The results presented in the paper are the means calculated across the 100 iterations.

5 Results

In this section, we evaluate the performance of BTM in detecting deepfakes in medical images. We start by comparing BTM to the baselines and analyze how well the method generalizes across different imaging machines (makes and manufacturers). Finally, we provide an ablation study on BTM to (1) confirm our hypothesis that forwards diffusion harms detection performance and (2) confirm that one step of backwards diffusion (i.e., $k = 1$) is ideal.

5.1 Baseline Analysis

In Table 1 we present the detection performance of two BTM detectors using different parameters (`init_features` of 8 and 32). The table shows that BTM outperforms the other baselines with a significant margin. This is regardless of whether the baseline was designed to detect semantic anomalies (e.g., the AE variants) or classical image forensic anomalies (Splice detectors and Satellite ViT). The exception to this observation is on the dataset (CTGAN-CT-Remove) where **all** of the methods fail, including BTM. For this dataset, every method obtains an AUC of about 0.55 which is essentially random guessing. We believe that the reason for this is that there are very few semantic anomalies left behind after a removal attack. Therefore, the models must rely on forensic anomalies alone to identify tampering (e.g., noise patterns). However, in this dataset, CT-GAN uses noise to further mask the removal of tumors. This is why BTM also struggles to identify the attack.

False positive rates are crucial in anomaly detection, particularly in the medical domain. To better understand the sensitivity of these algorithms, we plot their receiver operating characteristic (ROC) curves in Figure 4. The plot demonstrates that by adjusting the threshold of BTM, it is possible to achieve higher true positive rates with a very low false positive rate compared to other methods. Additionally, when stable diffusion is used to perform the attack, BTM can achieve a zero false positive rate.

5.2 Generalization

The medical images can be obtained using a wide variety of scanners from different manufactures. Each device may leave a different forensic signature or even capture the media with various levels

Table 1. Baselines comparison: The AUC of BTM compared to the baselines for each of the six attack scenarios. Bold values indicate the best result over 0.6 (close to random guessing).

	Injection			Removal		
	MRI	CT		MRI	CT	
	SD	CT-GAN	SD	SD	CT-GAN	SD
AE	0.80	0.56	0.79	0.91	0.45	0.93
In-Paint AE	0.52	0.80	0.76	0.65	0.60	0.56
OC-VAE	0.54	0.62	0.68	0.58	0.48	0.52
Unet-AE	0.63	0.46	0.71	0.73	0.48	0.92
Splice Buster	0.48	0.49	0.54	0.46	0.50	0.59
Splice Radar	0.55	0.73	0.61	0.62	0.57	0.65
Satellite ViT	0.54	0.61	0.65	0.63	0.47	0.51
OOD DDPM	0.50	0.54	0.53	0.63	0.42	0.49
BTM - 32 dim	0.99	0.81	0.91	0.98	0.55	0.86
BTM - 8 dim	0.93	0.69	0.87	0.93	0.52	0.94

of quality. Therefore, it is important to analyze the generalizability of BTM across different settings and scenarios, as opposed to looking at its average performance as a whole.

In our experiments, we used four different types of LightSpeed scanners and one type of Sensation scanner for the CT modality. For the MRI modality we used one type of scanner for Avanto and Optima, and two type of scanners for SIGNA. In Table 2 we provide the AUC and EER of each scanner for each dataset and attack. Our findings indicate that BTM is a robust detection method regardless of the imaging scanner or technology used. The only exception is in the case of the removal attack on CT scans, as previously explained.

Table 2. The performance of BTM when applied to images taken from different medical imaging devices.

SD-CT-Inject			CTGAN-CT-Inject			SD-MRI-Inject		
Scanner	AUC	EER	Scanner	AUC	EER	Scanner	AUC	EER
LightSpeed16	0.93	0.15	LightSpeed16	0.75	0.28	Avanto	0.92	0.20
Sensation 16	0.94	0.10	Sensation 16	0.96	0.10	Optima MR450w	1.00	0.00
LightSpeed Pro 16	0.93	0.18	LightSpeed Pro 16	0.90	0.18	SIGNA HDx	1.00	0.00
LightSpeed Ultra	0.85	0.22	LightSpeed Ultra	0.66	0.42	Signa HDxt	1.00	0.01
LightSpeed QX	0.89	0.17	LightSpeed QX	0.69	0.38			

SD-CT-Remove			CTGAN-CT-Remove			SD-MRI-Remove		
Scanner	AUC	EER	Scanner	AUC	EER	Scanner	AUC	EER
LightSpeed16	0.92	0.15	LightSpeed16	0.56	0.45	Avanto	0.97	0.09
Sensation 16	0.93	0.14	Sensation 16	0.56	0.44	Optima MR450w	1.00	0.02
LightSpeed Ultra	0.85	0.23	LightSpeed Ultra	0.58	0.44	SIGNA HDx	1.00	0.00
LightSpeed QX	0.78	0.28	LightSpeed QX	0.52	0.48	Signa HDxt	1.00	0.00

5.3 Ablation Study

In this section, we analyze the contribution of BTM’s direct backward diffusion step and other aspects which affect BTM’s performance.

5.3.1 *Eliminating Forwards Diffusion.* In section 3.2 we hypothesized that other diffusion based anomaly detectors fail because they perform forwards diffusion during the detection step. As a

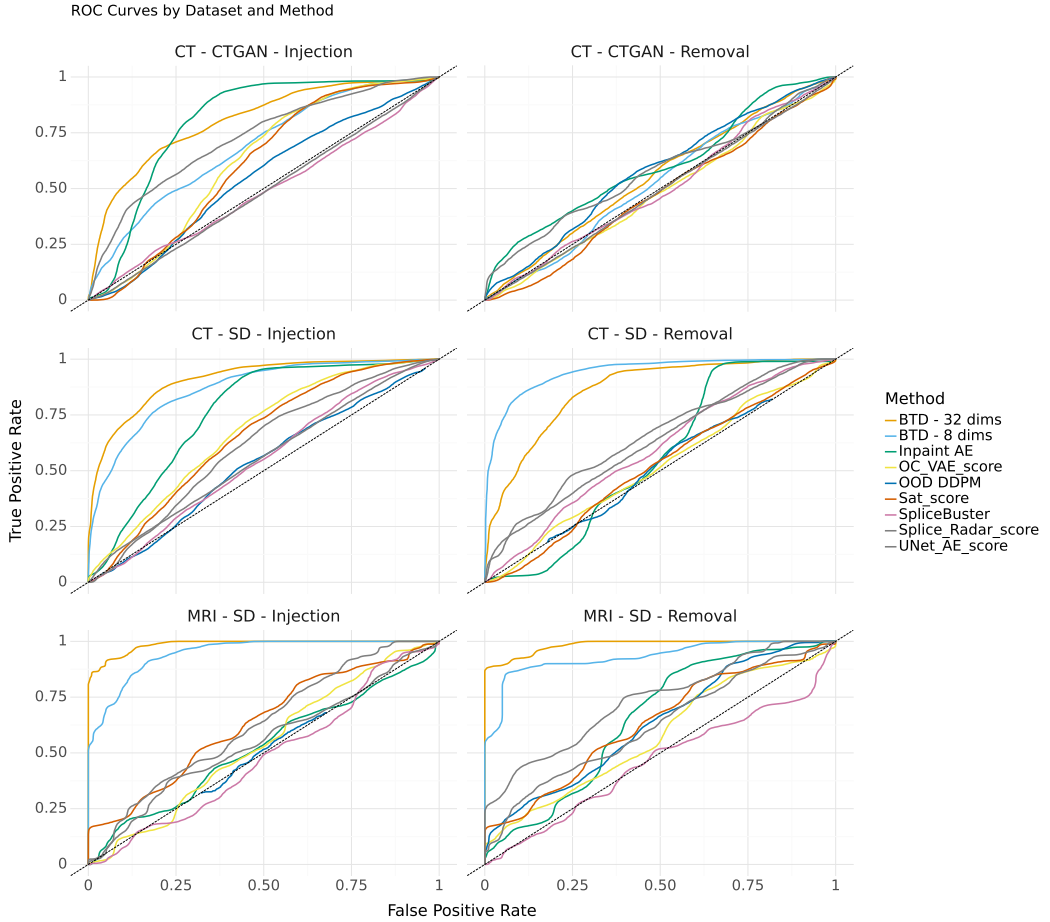


Fig. 4. ROC Curves of BTB and the baselines organized by dataset (attack scenario).

result, these methods generate irrelevant content during the backwards diffusion steps which leads to false positives and overpowers signatures of any subtle forensic evidence. However, BTB does not have this issue because it only performs backwards diffusion.

To validate this claim, we compare both approaches with increasing numbers of diffusion steps. We try in the backwards direction and we also try in both directions. Table 3 shows that in every case, applying the forwards diffusion process harms the results, even with a few steps. Therefore, performing only backward diffusion (BTB) is preferred. As discussed earlier, While the combine approach works well at identifying novel object and semantics, a fake cancer still appears as cancer. Thus, by performing backwards diffusion only, we have a better chance at detecting the tampering because we focus on the subtle forensics only such as distortions around the blending boundaries or latent noise patterns around the cancer.

To support this observation, we performed an empirical experiment to assess why the BTB residuals are more informative. We use an explainable AI tool called SHAP [27] to understand what anomaly would look at in both cases. SHAP's DeepExplainer provided insights into the

contributions of individual pixels (or regions) to the model's predictions. This allows us to visualize and quantify the significance of areas in the residual that contribute to the model's decision.

To conduct this experiment, we performed the following: from the MRI datasets SD-MRI-Inject and SD-MRI-Remove, we derived two different sets of residuals. The first was generated using the BTM approach ($|x_0 - x_{-1}|$), which involves only a single backward diffusion step. The second version performed 20 forward and then 20 backward steps, producing residuals ($|x_0 - x'_{-20}|$) for comparison. For each approach, we trained a convolutional neural network (CNN) to distinguish between real and fake residuals. These residuals were derived from images that the diffusion process had not encountered during training. We then ran the SHAP DeepExplainer tool on these residuals and analyzed the results.

Overall, we found that the SHAP values from the forwards-backwards approach yielded higher entropy compared to the BTM method. Specifically, the entropy of SHAP values for BTM residuals was 2.18 in the removal scenario and 2.20 in the injection scenario, whereas the entropy for forwards-backwards residuals averaged 2.94 for removal and 2.75 for injection. This indicates that the BTM method provides more informative insights overall, as lower entropy suggests more focused and interpretable contributions in the model's decision-making process.

A visual representation from this experiment supports our findings. Figure 5 demonstrates that the residuals from the BTM approach provide more concentrated information around the tampered areas (e.g., the center of the image). This focused interpretation aligns with BTM's objective of isolating forensic evidence indicative of tampering, enhancing its effectiveness in detecting manipulations. In contrast, the SHAP values from the forwards-backwards approach are more dispersed and less focused. This scattering suggests that the model struggles to identify relevant forensic features and instead relies on irrelevant noise and generated content. This unfocused behavior supports our hypothesis that the forward diffusion steps introduce redundant content, leading to less reliable anomaly detection and obscuring subtle evidence of tampering.

5.3.2 The Number of Backward Steps. The hyper-parameter d is the number of backward diffusion steps performed by BTM. In Figure 6 we plot its impact on detection performance for each of the datasets. We found that more than one backward diffusion step harms detection performance of both removal and injection attacks. In the case of detecting injections, further steps raise performance slightly but plateau at $d = 400$ and does not surpass $d = 1$. We believe this pattern is because there are some larger forensic patterns that take several iterations to remove. However, too many iterations prevents us from observing the subtle evidence in the residuals, leading to a decrease in performance.

In general, since $d = 1$ provides the best results, we recommend performing only one backward diffusion step when using BTM to detect forensic anomalies.

5.3.3 Forensic Evidence. It might be assumed that larger tampered areas would be easier to detect given the presence of more evidence. While this phenomenon exists in the CT injection datasets, in Figure 7 we show that the opposite is true for the MRI datasets. Upon further investigation, we found that SD tends to modify more of the image when the mask of the tumor is larger. This means that when larger masks are used, BTM has less contextual information to use to detect semantic anomalies. This is why larger tumors are slightly harder to detect than smaller ones for MRI compared to CT where the mask size is constant. In CT removal scenarios there is no correlation to tumor size because CTGAN always tampers the same sized area of $32 \times 32 \times 32$, regardless of how large the tumor was. Similarly, Uniform mask sizes of 32×32 were used to remove tumors in CT with Stable Diffusion as well.

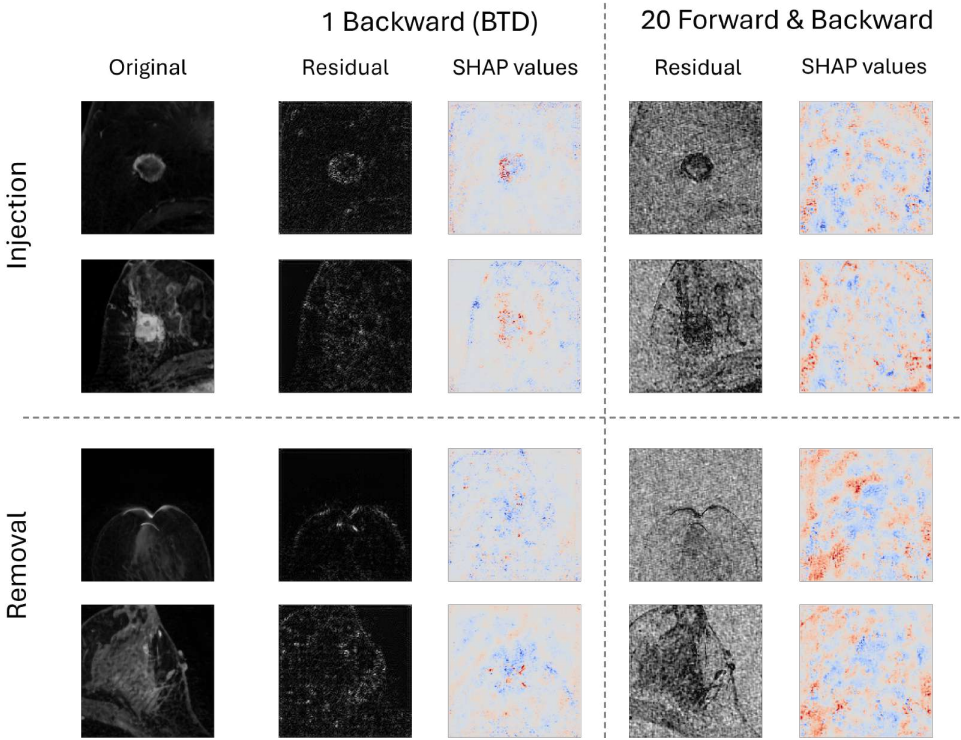


Fig. 5. BTD Explainability Experiment: BTD residuals and their SHAP values compared to residuals created with 20 F&B and their SHAP values

Table 3. Ablation Study: The impact forwards diffusion has on tamper detection. Existing methods perform both forwards and backwards (F&B) while BTD only performs backwards (B). The rows indicate the number of steps performed in the indicated direction(s) before measuring the residual. Bold values indicate the best result over 0.6 (close to random guessing).

		Injection			Removal		
		MRI SD	CT CT-G	SD	MRI SD	CT CT-G	SD
1	F&B	0.7279	0.6839	0.7375	0.8408	0.4828	0.6626
	B	0.9862	0.8056	0.9082	0.9838	0.5524	0.8607
10	F&B	0.5063	0.6502	0.6982	0.6755	0.4995	0.6086
	B	0.5873	0.6405	0.6909	0.6909	0.5061	0.6195
50	F&B	0.4047	0.6385	0.7062	0.6183	0.5059	0.6089
	B	0.4152	0.6130	0.6849	0.6058	0.5041	0.6081
100	F&B	0.3995	0.6331	0.7076	0.6025	0.4952	0.6064
	B	0.4015	0.5889	0.6895	0.5953	0.4974	0.5980
200	F&B	0.4266	0.6363	0.7231	0.6002	0.4930	0.5911
	B	0.4339	0.5685	0.6928	0.5942	0.4838	0.5754

Despite these observations, we see that fake tumors have consistently higher BTD-anomaly scores, regardless of their size. This supports our hypothesis that BTD focuses on subtle forensic evidence and not large semantic anomalies.

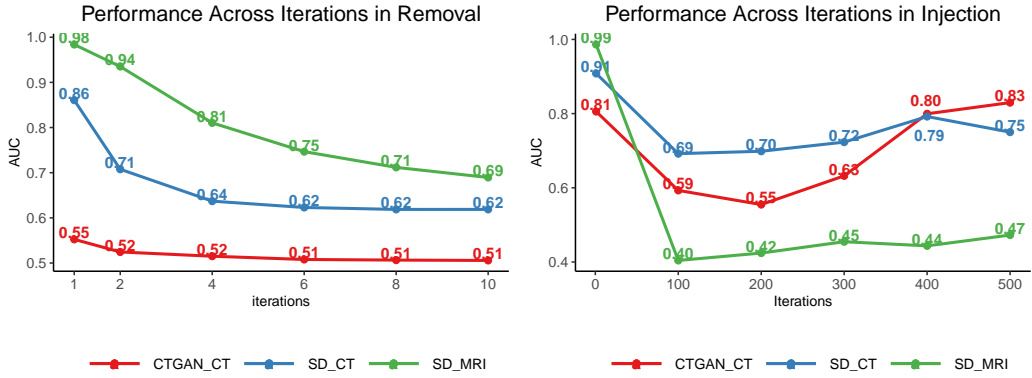


Fig. 6. The impact of diffusion step count on BTM performance for removal (left) and injection (right).

Tumor Size Analysis

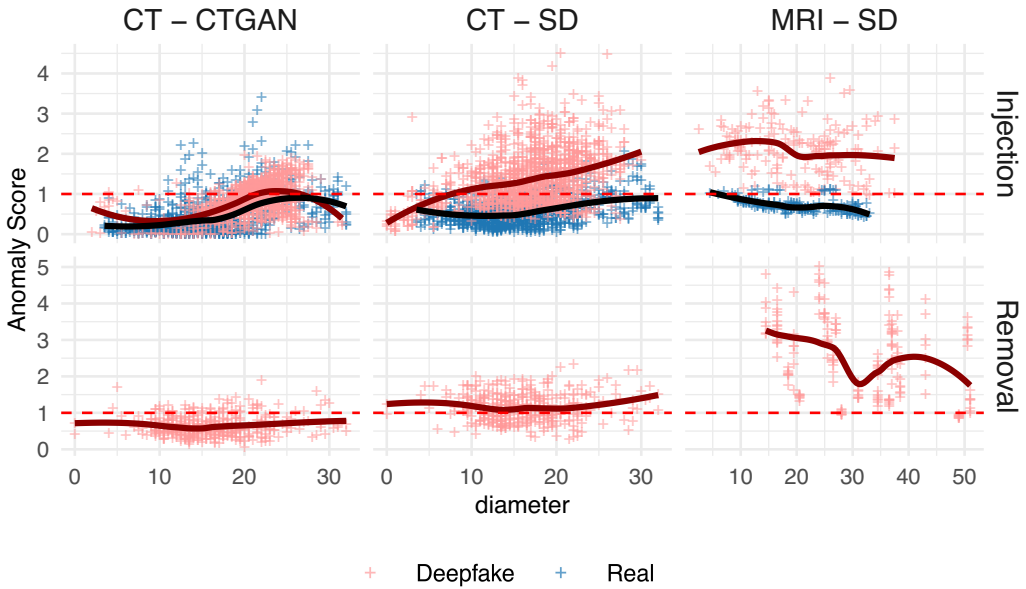


Fig. 7. The impact tumor size has on BTM detection performance. Anomaly scores are normalized to a false positive rate (FPR) of 0.1 (values over the red dashed line are anomalies). In datasets of removal (bottom row), real images (TB) are omitted as they lack tumors.

6 Conclusion

In this paper, we presented Back-in-Time Diffusion (BTM), a novel approach for identifying medical deepfakes. BTM surpasses current methodologies, establishing a new benchmark for detecting tampered medical images. It exhibits robustness across a diverse set of medical imaging modalities

(CT and MRI) and deepfake attacks (injection and removal). Moreover, the method's efficacy against different deepfake generation technologies (CT-GAN and SD) further underscores its adaptability and robustness. However, despite these achievements, challenges in deepfake detection still persist. For instance, BTM, along with all other methods, struggles to detect tumors that have been removed from CT images using CT-GAN. To assist the scientific community in addressing these challenges and to foster the development of solutions for combating medical deepfakes, we have made our datasets and source code openly accessible.⁴ Finally, as future work, it would be interesting to explore the application of BTM to other domains, such as classical image forensics.

Acknowledgments

This material is based upon work supported by the Zuckerman STEM Leadership Program. This project has received funding from the European Union's Horizon 2020 research and innovation programme under grant agreement 952172.



References

- [1] Steve Adler. 2023. East River Medical Imaging Cyberattack Affects 606,000 Patients. <https://www.hipaajournal.com/east-river-medical-imaging-cyberattack-affects-606000-patients/>. (Accessed on 07/30/2024).
- [2] Zahid Akhtar. 2023. Deepfakes Generation and Detection: A Short Survey. *Journal of Imaging* 9, 1 (2023), 18.
- [3] SG Armato III, G McLennan, L Bidaut, MF McNitt-Gray, CR Meyer, AP Reeves, B Zhao, DR Aberle, CI Henschke, EA Hoffman, et al. 2015. Data from LIDC-IDRI [data set]. *The Cancer Imaging Archive* 10 (2015), K9.
- [4] Christiaan Beek. 2018. McAfee researchers find poor security exposes medical data to cybercriminals. *McAfee Blogs* (2018).
- [5] Mo Chen, Jessica Fridrich, Miroslav Goljan, and Jan Lukás. 2008. Determining image origin and integrity using sensor noise. *IEEE Transactions on information forensics and security* 3, 1 (2008), 74–90.
- [6] Davide Cozzolino, Francesco Marra, Giovanni Poggi, Carlo Sansone, and Luisa Verdoliva. 2017. PRNU-based forgery localization in a blind scenario. In *Image Analysis and Processing-ICIAP 2017: 19th International Conference, Catania, Italy, September 11-15, 2017, Proceedings, Part II 19*. Springer, 569–579.
- [7] Davide Cozzolino, Giovanni Poggi, and Luisa Verdoliva. 2015. Splicebuster: A new blind image splicing detector. In *2015 IEEE International Workshop on Information Forensics and Security (WIFS)*. IEEE, 1–6.
- [8] Davide Cozzolino and Luisa Verdoliva. 2019. Noiseprint: A CNN-based camera model fingerprint. *IEEE Transactions on Information Forensics and Security* 15 (2019), 144–159.
- [9] Antonia Creswell, Tom White, Vincent Dumoulin, Kai Arulkumaran, Biswa Sengupta, and Anil A Bharath. 2018. Generative adversarial networks: An overview. *IEEE signal processing magazine* 35, 1 (2018), 53–65.
- [10] Florinel-Alin Croitoru, Vlad Hondru, Radu Tudor Ionescu, and Mubarak Shah. 2023. Diffusion models in vision: A survey. *IEEE Transactions on Pattern Analysis and Machine Intelligence* (2023).
- [11] Alexey Dosovitskiy, Lucas Beyer, Alexander Kolesnikov, Dirk Weissenborn, Xiaohua Zhai, Thomas Unterthiner, Mostafa Dehghani, Matthias Minderer, Georg Heigold, Sylvain Gelly, et al. 2020. An image is worth 16x16 words: Transformers for image recognition at scale. *arXiv preprint arXiv:2010.11929* (2020).
- [12] Marco Eichelberg, Klaus Kleber, and Marc Kämmerer. 2020. Cybersecurity in PACS and medical imaging: an overview. *Journal of Digital Imaging* 33, 6 (2020), 1527–1542.
- [13] Guy Frankovits and Yisroel Mirsky. 2023. Discussion Paper: The Threat of Real Time Deepfakes. *arXiv preprint arXiv:2306.02487* (2023).
- [14] Aurobrata Ghosh, Zheng Zhong, Terrance E Boulton, and Maneesh Singh. 2019. SpliceRadar: A Learned Method For Blind Image Forensics.. In *CVPR Workshops*. 72–79.
- [15] Ian Goodfellow, Jean Pouget-Abadie, Mehdi Mirza, Bing Xu, David Warde-Farley, Sherjil Ozair, Aaron Courville, and Yoshua Bengio. 2020. Generative adversarial networks. *Commun. ACM* 63, 11 (2020), 139–144.
- [16] Joseph Goodier and Neill DF Campbell. 2023. Likelihood-based Out-of-Distribution Detection with Denoising Diffusion Probabilistic Models. *arXiv preprint arXiv:2310.17432* (2023).

⁴Redacted due to the double-blind review policy.

- [17] Mark S Graham, Walter HL Pinaya, Petru-Daniel Tudosiu, Parashkev Nachev, Sebastien Ourselin, and Jorge Cardoso. 2023. Denoising diffusion models for out-of-distribution detection. In *Proceedings of the IEEE/CVF Conference on Computer Vision and Pattern Recognition*. 2947–2956.
- [18] Matthias Haselmann, Dieter P Gruber, and Paul Tabatabai. 2018. Anomaly detection using deep learning based image completion. In *2018 17th IEEE international conference on machine learning and applications (ICMLA)*. IEEE, 1237–1242.
- [19] Jonathan Ho, Ajay Jain, and Pieter Abbeel. 2020. Denoising diffusion probabilistic models. *Advances in neural information processing systems* 33 (2020), 6840–6851.
- [20] János Horváth, Sriram Baireddy, Hanxiang Hao, Daniel Mas Montserrat, and Edward J Delp. 2021. Manipulation detection in satellite images using vision transformer. In *Proceedings of the IEEE/CVF Conference on Computer Vision and Pattern Recognition*. 1032–1041.
- [21] Minyoung Huh, Andrew Liu, Andrew Owens, and Alexei A Efros. 2018. Fighting fake news: Image splice detection via learned self-consistency. In *Proceedings of the European conference on computer vision (ECCV)*. 101–117.
- [22] Byan Ke. 2022. Singaporean man’s face ends up in deepfake porn after he refuses to pay hacker \$5,800. <https://news.yahoo.com/singaporean-mans-face-ends-deepfake-171743924.html>. (Accessed on 08/30/2023).
- [23] Hasam Khalid and Simon S Woo. 2020. OC-FakeDect: Classifying deepfakes using one-class variational autoencoder. In *Proceedings of the IEEE/CVF conference on computer vision and pattern recognition workshops*. 656–657.
- [24] Dahun Kim, Sanghyun Woo, Joon-Young Lee, and In So Kweon. 2019. Deep video inpainting. In *Proceedings of the IEEE/CVF Conference on Computer Vision and Pattern Recognition*. 5792–5801.
- [25] Paweł Korus and Jiwu Huang. 2016. Multi-scale analysis strategies in PRNU-based tampering localization. *IEEE Transactions on Information Forensics and Security* 12, 4 (2016), 809–824.
- [26] Victor Livermoche, Vineet Jain, Yashar Hezaveh, and Siamak Ravanbakhsh. 2023. On Diffusion Modeling for Anomaly Detection. *arXiv preprint arXiv:2305.18593* (2023).
- [27] Scott Lundberg. 2017. A unified approach to interpreting model predictions. *arXiv preprint arXiv:1705.07874* (2017).
- [28] Siwei Lyu, Xunyu Pan, and Xing Zhang. 2014. Exposing region splicing forgeries with blind local noise estimation. *International journal of computer vision* 110 (2014), 202–221.
- [29] Hannes Mareen, Dante Vanden Bussche, Fabrizio Guillaro, Davide Cozzolino, Glenn Van Wallendael, Peter Lambert, and Luisa Verdoliva. 2022. Comprint: Image forgery detection and localization using compression fingerprints. In *International Conference on Pattern Recognition*. Springer, 281–299.
- [30] Yisroel Mirsky and Wenke Lee. 2021. The creation and detection of deepfakes: A survey. *ACM Computing Surveys (CSUR)* 54, 1 (2021), 1–41.
- [31] Yisroel Mirsky, Tom Mahler, Ilan Shelef, and Yuval Elovici. 2019. {CT-GAN}: Malicious tampering of 3d medical imagery using deep learning. In *28th USENIX Security Symposium (USENIX Security 19)*. 461–478.
- [32] Arian Mousakhan, Thomas Brox, and Jawad Tayyub. 2023. Anomaly Detection with Conditioned Denoising Diffusion Models. *arXiv preprint arXiv:2305.15956* (2023).
- [33] Alessandro Piva. 2013. An overview on image forensics. *International Scholarly Research Notices* 2013 (2013).
- [34] Aditya Ramesh, Mikhail Pavlov, Gabriel Goh, Scott Gray, Chelsea Voss, Alec Radford, Mark Chen, and Ilya Sutskever. 2021. Zero-shot text-to-image generation. In *International Conference on Machine Learning*. PMLR, 8821–8831.
- [35] Robin Rombach, Andreas Blattmann, Dominik Lorenz, Patrick Esser, and Björn Ommer. 2022. High-Resolution Image Synthesis With Latent Diffusion Models. In *Proceedings of the IEEE/CVF Conference on Computer Vision and Pattern Recognition (CVPR)*. 10684–10695.
- [36] Olaf Ronneberger, Philipp Fischer, and Thomas Brox. 2015. U-net: Convolutional networks for biomedical image segmentation. In *Medical Image Computing and Computer-Assisted Intervention—MICCAI 2015: 18th International Conference, Munich, Germany, October 5–9, 2015, Proceedings, Part III 18*. Springer, 234–241.
- [37] Nataniel Ruiz, Yuanzhen Li, Varun Jampani, Yael Pritch, Michael Rubinstein, and Kfir Aberman. 2023. Dreambooth: Fine tuning text-to-image diffusion models for subject-driven generation. In *Proceedings of the IEEE/CVF Conference on Computer Vision and Pattern Recognition*. 22500–22510.
- [38] Ashirbani Saha, Michael R Harowicz, Lars J Grimm, Jingxi Weng, EH Cain, CE Kim, SV Ghate, R Walsh, and Maciej A Mazurowski. 2021. Dynamic contrast-enhanced magnetic resonance images of breast cancer patients with tumor locations [Data set]. *The Cancer Imaging Archive* (2021).
- [39] Nahian Siddique, Sidike Paheding, Colin P Elkin, and Vijay Devabhaktuni. 2021. U-net and its variants for medical image segmentation: A review of theory and applications. *Ieee Access* 9 (2021), 82031–82057.
- [40] Po-Chyi Su, Bo-Hong Huang, and Tien-Ying Kuo. 2024. UFCC: A Unified Forensic Approach to Locating Tampered Areas in Still Images and Detecting Deepfake Videos by Evaluating Content Consistency. *Electronics* 13, 4 (2024), 804.
- [41] Luisa Verdoliva. 2020. Media forensics and deepfakes: an overview. *IEEE journal of selected topics in signal processing* 14, 5 (2020), 910–932.
- [42] Xin Wang, Hui Guo, Shu Hu, Ming-Ching Chang, and Siwei Lyu. 2022. Gan-generated faces detection: A survey and new perspectives. *arXiv preprint arXiv:2202.07145* (2022).

- [43] Zack Wittaker. 2020. A billion medical images are exposed online, as doctors ignore warnings | TechCrunch. <https://techcrunch.com/2020/01/10/medical-images-exposed-pacs/>. (Accessed on 11/06/2021).
- [44] Julia Wolleb, Florentin Bieder, Robin Sandkühler, and Philippe C Cattin. 2022. Diffusion models for medical anomaly detection. In *International Conference on Medical image computing and computer-assisted intervention*. Springer, 35–45.
- [45] Yue Wu, Wael Abd-Almageed, and Prem Natarajan. 2018. Busternet: Detecting copy-move image forgery with source/target localization. In *Proceedings of the European conference on computer vision (ECCV)*. 168–184.
- [46] Jie Yang, Ruijie Xu, Zhiqian Qi, and Yong Shi. 2021. Visual anomaly detection for images: A survey. *arXiv preprint arXiv:2109.13157* (2021).
- [47] Chong Zhou and Randy C Paffenroth. 2017. Anomaly detection with robust deep autoencoders. In *Proceedings of the 23rd ACM SIGKDD international conference on knowledge discovery and data mining*. 665–674.